

## Crystal structures of two partially dehydrated chlorites: The “modified” chlorite structure

STEPHEN GUGGENHEIM AND WUDI ZHAN

Department of Earth and Environmental Sciences, University of Illinois at Chicago, 845 West Taylor Street, Chicago, Illinois 60607, U.S.A.

### ABSTRACT

Chromian clinochlore-*IIb-4* (triclinic) and *IIb-2* (monoclinic) polytypes from the Day Book Body, North Carolina, were heated to 650 °C for 5 hours and air quenched. Single-crystal X-ray refinements of the (metastable) product phases resulted in  $R = wR = 0.056$  and  $R = wR = 0.061$  for the triclinic and monoclinic forms, respectively. The heat-treated triclinic form has  $C\bar{1}$  symmetry and cell parameters  $a = 5.368(1)$ ,  $b = 9.297(2)$ ,  $c = 14.215(6)$  Å,  $\alpha = 89.86(3)$ ,  $\beta = 97.15(3)$ ,  $\gamma = 89.98(2)^\circ$ , and  $V = 703.95(36)$  Å<sup>3</sup>, and the monoclinic form has  $a = 5.372(1)$ ,  $b = 9.291(2)$ ,  $c = 14.270(7)$  Å,  $\beta = 97.34(3)^\circ$ , and  $V = 706.4(4)$  Å<sup>3</sup> in  $C2/m$  symmetry. The product structures are topotactic with the parent phases, with the 2:1 layer of the product nearly identical to that of the parent. Dehydroxylation of the interlayer of the parent produces two quasi-planar sets of atoms between adjacent 2:1 layers. Although, based on the refinement of the average structure, the cations and anions are apparently disordered in these planes, cations (Mg, Al, Cr) must have three oxygen atom nearest neighbors and oxygen atoms must be coordinated to three cations. Apparent disorder is related to lateral displacements of the interlayer planes within the (001) plane. Interlayer-site to interlayer-site distances are near 1.8 Å. Second nearest-neighbor distances for most of the interlayer sites are short, near 2.3 Å. A model is proposed where, at high temperatures, the interlayer planes become more extended and planar, but the planes “crumple” upon cooling to more closely approach higher-order nearest-neighbor atoms. These changes upon cooling might be a significant driving force for additional cation and anion ordering in the interlayer, since the interlayer sites have very different second nearest-neighbor environments. Thus, with appropriate cooling rates, cation ordering possibly may be obtained. However, the development of an ordered pattern of cations and anions may also be dependent on kinetics; decomposition is favored over time because of the instability of threefold-coordinated interlayer ions.

### INTRODUCTION

Brindley and Ali (1950) observed that dehydroxylation of the interlayer of chlorite occurs when chlorite is heated in air near 550 °C for about an hour. They referred to the product as the “modified chlorite” structure, which they found to be remarkably persistent, even for dehydroxylated samples that are immersed in water for long periods. The chlorite to “modified chlorite” reaction is utilized by clay mineralogists (e.g., Moore and Reynolds 1989) to determine the presence of Fe,Mg-rich chlorite in a mixture possibly containing 7 Å phyllosilicates (i.e., kaolin-serpentine minerals). In X-ray powder patterns of samples containing oriented grains of chlorite with moderate to high Fe contents, the 001 peak may not be present or, if present, very weak in intensity, but the higher-order peaks can be relatively strong. These higher-order peaks superpose over possible 7 Å phyllosilicate peaks. To discriminate between the presence or absence of Fe,Mg-rich chlorite in this mixture, the oriented clay mineral aggregate is heated for one hour at 550 °C to produce “modified chlorite,” which characteristically has a strong 001 peak ( $d$ -value = 14 Å), nearly absent 002 ( $d$ -value = 7 Å) and 003 peaks, either a weak or absent 004 peak de-

pending on composition, and a weak 005 peak. Thus, after heating, the presence of chlorite is revealed if the X-ray pattern of the sample shows a 14 Å peak, and the presence of 7 Å phyllosilicates is indicated if a 7 Å peak occurs.

On further examination of heat-treated Mg-, Al-, and Fe-rich clinochlores, Brindley and Chang (1974) used an X-ray powder diffractometer to identify a 27 Å spacing in oriented aggregates. They noted also that the width of the 001 ( $d$ -value = 27 Å) and 003 peaks ( $d$ -value = 9 Å) differ from that of the 002 peak ( $d$ -value = 14 Å), and that the 002 spacing is not a precise multiple of the 001 spacing. Brindley and Chang (1974) and later workers (e.g., Villieras et al. 1994) assumed that these results were related to a single phase in the heat-treated sample. However, Zhan and Guggenheim (1995) were able to obtain similar results from a single crystal of chlorite by heating it slowly to 650 °C in air and then maintaining temperature for 24 hours. Single crystal, X-ray examination showed two product phases with a topotactic relationship, with each  $c$  axis parallel. One phase is well crystallized and has sharp reflections. This phase maintains the basic 2:1 layer structure with a repeat of 14 Å. The second phase has a 27 Å repeat and is very poorly crystallized; Zhan and Guggenheim (1995) could locate only about 15 weak and diffuse reflections from this phase. Zhan and Guggenheim (1995) determined that the fugacity of water is an important vari-

\*E-mail: xtal@uic.edu

able in the formation of the 27 Å phase, although the polytype arrangement and octahedral character of the 2:1 layer of the initial chlorite may be important variables also. Bai et al. (1993) determined the metastable phase relations involving chlorite and the "modified chlorite" phase, and Nelson and Guggenheim (1993) studied the effects of heating chlorite to temperatures just below dehydroxylation.

Zhan and Guggenheim (1995) retained the term "modified chlorite" to describe the 14 Å chlorite-like material with a dehydroxylated interlayer region, whereas the "27 Å phase" refers to the poorly crystalline material with a 27 Å repeat. In this study, we report on the crystal structure of "modified chlorite." Two structures are reported, one based on a chlorite with monoclinic symmetry and the other with triclinic symmetry prior to heating.

## EXPERIMENTAL METHODS

### Samples

X-ray precession methods were used to find a suitable single crystal of chromian clinochlore-*Iib*-4 from the Day Book Body, North Carolina, for further study. The crystal is triclinic and is from the same specimen used in structural studies by Phillips et al. (1980) and Nelson and Guggenheim (1993). The material has a low Fe content and a structural formula of  $(\text{Mg}_{2.97}\text{Al}_{0.03})(\text{Si}_{3.02}\text{Al}_{0.98})\text{O}_{10}(\text{OH})_2(\text{Mg}_{1.98}\text{Al}_{0.69}\text{Cr}_{0.23}\text{Fe}_{0.04}^{3+}\text{Fe}_{0.04}^{2+}\text{Ni}_{0.02})(\text{OH})_6$ . The crystal of clinochlore-*Iib*-4 was approximately  $0.32 \times 0.24 \times 0.10$  mm in size. An additional crystal from the same sample, with a size of  $0.23 \times 0.17 \times 0.27$  mm, was found to be a monoclinic clinochlore-*Iib*-2 polytype. Both crystals exhibited sharp reflections without the streaking commonly indicative of stacking disorder.

### Heating experiments/space group

Each crystal was heated in a furnace from a cold start. After reaching the 650 °C set temperature, heating was continued for 5 hours. Precession photographs showed that the crystals had been transformed to modified chlorite, reflections were free from any streaking, and each crystal appeared to be of one polytype. The absence of  $h + k = 2n + 1$  reflections in the precession photographs of each crystal showed that both have *C*-centered unit cells. It was assumed that the heat-treated *Iib*-4 polytype has  $C\bar{1}$  symmetry and, based on an apparent mirror plane and a twofold axis, that the material derived from the *Iib*-2 polytype has *C2/m* symmetry. We examined these assumptions after completion of the refinement because of the possibility that the space-group symmetry might be described more properly in a subgroup, especially considering that there is potential for cation and anion ordering in the interlayer (see discussion). With reduced symmetry from a pattern of cation and anion ordering, however, possible ordering schemes would place cations next to cations in the interlayer, which is unlikely. Thus, we believe that the use of centric space groups for refinement was justified.

In both crystals, reflections at low  $2\theta$  are sharp, but reflections at higher  $2\theta$  exhibit apparent dispersion effects (general broadening of reflections and an increase in apparent mosaic spread). Each of the two heat-treated samples showed crystal edges damaged in the heating process, perhaps by the escape

of H<sub>2</sub>O. Such damage, which affects the orientation of layers at the outer crystal margin more than in the bulk of the crystal, produces greater diffuseness of higher  $2\theta$  reflections relative to the lower angle data. Thus, reflections above  $l > 10$  become difficult to measure precisely.

### Data collection

An automated Picker four-circle, single-crystal X-ray diffractometer was used with graphite monochromatized MoK $\alpha$  radiation for data measurement. For the heat-treated *Iib*-4 polytype, a least-squares refinement of 112 medium-angle reflections (14 reflections in eight octants) resulted in cell parameters of  $a = 5.368(1)$ ,  $b = 9.297(2)$ ,  $c = 14.215(6)$  Å,  $\alpha = 89.86(3)$ ,  $\beta = 97.15(3)$ ,  $\gamma = 89.98(2)^\circ$ , and  $V = 703.95(36)$  Å<sup>3</sup>. Least-squares refinement of 144 medium-to-high angle reflections (18 reflections in 8 octants) for the heat-treated *Iib*-2 polytype resulted in  $a = 5.372(1)$ ,  $b = 9.291(2)$ ,  $c = 14.270(7)$  Å,  $\beta = 97.34(3)$ , and  $V = 706.4(4)$  Å<sup>3</sup>. Both data sets were obtained for four octants of the limiting sphere sampled in the range  $h = 0$  to 6,  $k = -12$  to 12, and  $l = -10$  to 10, with a scan rate of 1.0°/min, scan window of 2.5°, and background time of one half the scan time. The  $2\theta:\theta$  scan mode was used with three standard reflections monitored every 360 min (approximately every 60 reflections) for electronic stability. Reflections were considered observed if intensity,  $I$ ,  $> 5\sigma$ , where  $\sigma(I) = [Ct + 0.25(t_c/t_b)^2(B_1+B_2)+PI]^2$ <sup>1,\*2</sup>, and  $Ct$  is the total integrated count in time  $t_c$ ,  $B_1$ , and  $B_2$  are the background counts in time  $t_b$ , and  $p$ , the estimate of the standard error, = 0.03. Lorentz-polarization corrections were made for each sample. Absorption effects for the heat-treated *Iib*-4 polytype were corrected using ten different *hkl* reflections involving a total of 230 measurements using a  $\Psi$ -scan method (Siemens 1990) to define a set of equations for correction, and similar corrections were made for the heat-treated *Iib*-2 polytype with 12 *hkl* reflections involving 280 individual measurements. Of the 1207 reflections measured for the heat-treated *Iib*-4 polytype, 934 unique non-zero reflections were produced after symmetry averaging. For the heat-treated *Iib*-2 polytype, there was a total of 1305 reflections measured, resulting in 517 unique nonzero reflections after symmetry averaging.

### Structure determination and refinement

For the heat-treated *Iib*-4 polytype, the atomic parameters (Nelson and Guggenheim 1993) for atoms in the 2:1 layer were used as initial parameters. Scattering factor curves were calculated using the method of Sales (1987) and the tables of Cromer and Mann (1968), assuming half-ionization of atoms. The least-squares refinement program "Shelxtl Plus" (Siemens 1990) was used, and the reflections were assigned unit weights and a single scale factor. No attempt was made to remove any data that may have resulted from the 27 Å phase because the reflections from this phase were very few in number, very weak, and generally did not overlap or occur near the reflections being collected (Zhan and Guggenheim 1995). With the scale factor, atomic coordinates  $x$ ,  $y$ ,  $z$ , and isotropic displacement factors allowed to vary, the  $R_w$  equaled 0.224. Fourier electron-density maps were made and four unique peaks were found in the interlayer ( $z$  coordinates from 0.38 to 0.62). These peaks were of equal

height (five electrons) and were suggestive of one-half occupancy of Mg or O. Initially, peaks were assigned as Mg or O, but subsequent refinement suggested a split atom model. The  $R_w$  factor was 0.113 at this stage of refinement.

Additional Fourier electron density maps were made and anomalous peaks at the levels of the tetrahedral cations occurred at  $x = 0.233$ ,  $y = 0.833$ ,  $z = 0.199$  and at their symmetry-related equivalent positions. These peaks were interpreted as occurring from 2:1 layer shifts of  $\pm b/3$ , which relate to a random interlayering of 2:1 layers. To simulate the intergrowth (i.e., domains) of the two positions of 2:1 layers, four additional T atoms of partial occupancy (15%) were added [based on refinement results, these coordinates are,  $x, y, z$ : 0.231(4), 0.833(3), 0.200(2); 0.194(6), 0.677(6), 0.217(6); 0.543(6), 0.443(6), 0.200(6); 0.008(6), 0.056(6), 0.256(5)]. Basal oxygen atoms of the intergrowth were not observed and would be expected to be below background. Octahedral cations of the intergrowth, which also repeat at intervals of  $\pm b/3$ , superpose over the octahedral cations of the *I1b*-4 form. Multiplicities of atoms that coincided with the *I1b*-4 stacking sequence were set at 1.15; these included all apical oxygen, OH in the 2:1 layer, and M cations. After several cycles, the  $R_w$  factor dropped to 0.093. Anisotropic displacement factors were allowed to vary for all atoms of the triclinic form and one T site relating uniquely to the intergrowths. Refinement results for the modified triclinic clinoclone structure are  $R = 0.056$  and  $R_w = 0.056$ , with 183 varied parameters, where  $R_w = [\sum_w(|F_o| - |F_c|)^2 / \sum_w |F_c|^2]^{1/2}$ . A final difference-Fourier density map was flat.

The initial values of the atomic parameters of the atoms of the 2:1 layer for the heat-treated *I1b*-2 polytype were those reported by Zheng and Bailey (1989). The procedures used to refine the structure were similar to those described above. Af-

ter several cycles in which the scale factor, atomic coordinates  $x, y, z$ , and isotropic displacement factors were varied, the  $R_w$  equaled 0.217. Fourier electron density maps revealed six unique peaks in the interlayer ( $z = 0.38$  to  $0.60$ ), and these peaks were interpreted as relating to half-occupied Mg + O sites. The  $R_w$  value was 0.165 after these sites were included in the refinement, and further refinement reduced the value to 0.113. Difference electron density maps revealed additional peaks at the  $z$ -level of tetrahedral cations at  $x = 0.234$ ,  $y = 0.500$ ,  $z = 0.201$  and symmetry-related sites, which were interpreted as occurring from  $\pm b/3$  layer shifts of some of the 2:1 layers. The refinement procedure proceeded as above by including these additional peaks [after refinement, these coordinates are,  $x, y, z$ : 0.235(4), 0.5, 0.202(2); 0.211(7), 0.358(6), 0.227(6); 0.496(7), 0.543(6), 0.227(6)], with partial occupancy of 0.10. Multiplicities of 1.10 were assigned to atoms of the 2:1 layer that were coincident with atoms of the interlayering domains. After several cycles, the  $R_w$  factor dropped to 9.73%. Anisotropic displacement factors were allowed to vary for all atoms of the monoclinic phase and one atom that can be attributed to the domains of displaced 2:1 layers. Refinement results for the modified monoclinic clinoclone structure are  $R = 0.061$  and  $R_w = 0.061$ , with 108 varied parameters. A difference map obtained at this stage was flat. Final atomic and displacement factors for both data sets are listed in Table 1, and bond lengths and select bond angles are listed in Table 2.

## DISCUSSION

The refined Day-Book chlorite structure is consistent with the interlayer structure being completely dehydroxylated. The decomposition of the interlayer can be represented as follows:  $R_3(\text{OH})_6 = R_3\text{O}_3 + 3\text{H}_2\text{O}$ , where  $R$  represents the interlayer cat-

TABLE 1. Atomic coordinates and displacement factors for modified chlorite

Atom	$x$	$y$	$z$	$U_{eq}$	$U_{11}$	$U_{22}$	$U_{33}$	$U_{23}$	$U_{13}$	$U_{12}$
<b>Triclinic modified chlorite</b>										
M1	0.0000	0.0000	0.0000	0.032(1)	0.004(1)	0.008(1)	0.084(3)	0.001(1)	0.010(1)	-0.0029(8)
M2	0.0005(3)	0.3336(2)	-0.0002(2)	0.0334(9)	0.0059(8)	0.0097(8)	0.086(2)	-0.0003(9)	0.010(1)	-0.0023(6)
T1	0.2297(3)	0.1662(2)	0.1933(2)	0.036(1)	0.0119(9)	0.0161(9)	0.081(3)	0.001(1)	0.009(1)	-0.0024(6)
T2	0.2311(3)	0.4989(2)	0.1934(2)	0.035(1)	0.0119(9)	0.0175(9)	0.077(3)	0.001(1)	0.010(1)	-0.0016(7)
O1	0.1920(7)	0.1662(4)	0.0767(5)	0.035(2)	0.009(2)	0.013(2)	0.684(4)	0.000(2)	0.010(2)	-0.003(1)
O2	0.6924(7)	-0.0005(4)	0.0775(4)	0.038(2)	0.011(2)	0.014(2)	0.088(4)	-0.002(2)	0.008(2)	-0.002(1)
O3	0.208(1)	0.3321(6)	0.2348(6)	0.064(2)	0.044(3)	0.027(2)	0.118(5)	0.003(3)	0.002(3)	-0.003(2)
O4	0.513(1)	0.1010(6)	0.2344(6)	0.060(2)	0.025(3)	0.048(3)	0.112(5)	0.012(3)	0.020(3)	0.008(2)
O5	0.013(1)	0.0652(8)	0.2338(7)	0.053(2)	0.023(3)	0.048(3)	0.097(5)	-0.009(3)	0.020(3)	-0.022(2)
O6=OH	0.6919(7)	0.3326(4)	0.0754(5)	0.041(2)	0.012(2)	0.015(2)	0.099(4)	-0.000(2)	0.011(2)	-0.002(1)
I1	0.186(2)	0.333(2)	0.575(1)	0.087(3)	0.072(5)	0.085(5)	0.105(6)	0.004(5)	0.017(5)	0.001(5)
I2	0.194(2)	-0.005(1)	0.574(1)	0.080(3)	0.075(5)	0.067(5)	0.098(6)	0.000(5)	0.013(5)	0.003(4)
I3	0.198(2)	0.666(1)	0.597(1)	0.093(3)	0.072(5)	0.076(5)	0.135(6)	-0.006(5)	0.022(5)	-0.007(5)
I4	0.129(1)	0.6660(9)	0.3874(9)	0.062(2)	0.025(3)	0.030(3)	0.132(5)	-0.002(4)	0.015(4)	-0.004(3)
I5	0.138(1)	0.3338(9)	0.410(1)	0.081(2)	0.022(3)	0.029(3)	0.193(6)	0.004(4)	0.014(4)	0.002(3)
I6	0.138(1)	0.0018(8)	0.411(1)	0.085(2)	0.026(3)	0.026(3)	0.207(6)	-0.011(4)	0.035(4)	-0.002(3)
<b>Monoclinic modified chlorite</b>										
M1	0.0000	0.0000	0.0000	0.039(1)	0.013(1)	0.007(1)	0.096(4)	0.0000	0.003(2)	0.0000
M2	0.0000	0.3331(2)	0.0000	0.040(1)	0.015(1)	0.0080(9)	0.098(3)	0.0000	0.002(1)	0.0000
T1	0.2323(3)	0.1673(2)	0.1934(2)	0.0448(9)	0.0238(7)	0.0163(7)	0.093(3)	0.0006(9)	0.0022(8)	0.0005(5)
O1	0.1937(6)	0.1668(3)	0.0768(4)	0.047(2)	0.020(2)	0.015(1)	0.105(4)	0.001(2)	0.002(2)	0.000(1)
O2	0.208(1)	0.0000	0.2357(7)	0.067(2)	0.058(4)	0.022(3)	0.116(6)	0.0000	-0.011(4)	0.0000
O3	0.5145(9)	0.2303(5)	0.2351(5)	0.077(2)	0.043(2)	0.047(3)	0.140(5)	-0.008(3)	0.010(3)	-0.012(2)
O4=OH	0.1909(9)	0.5000	0.0752(6)	0.054(2)	0.020(2)	0.014(2)	0.127(5)	0.0000	0.004(3)	0.0000
I1	0.129(1)	0.0000	0.388(1)	0.079(3)	0.042(4)	0.044(4)	0.151(6)	0.0000	0.007(4)	0.0000
I2	0.195(2)	0.664(1)	0.5747(9)	0.097(3)	0.089(5)	0.084(5)	0.110(6)	0.007(5)	-0.013(5)	-0.004(4)
I3	0.133(1)	0.3321(6)	0.4096(8)	0.097(2)	0.041(3)	0.038(3)	0.215(6)	0.013(4)	0.025(4)	0.003(2)
I4	0.198(3)	0.0000	0.596(1)	0.101(3)	0.103(6)	0.088(6)	0.106(6)	0.0000	-0.004(5)	0.0000

Note: Displacement parameters are of the form  $\exp[-2\pi^2(U_{11}h^2a^{*2} + U_{22}k^2b^{*2} + U_{33}l^2c^{*2} + 2U_{12}hka^*b^* + 2U_{13}hla^*c^* + 2U_{23}klb^*c^*)]$ .

**TABLE 2a.** Select interatomic distances and angles for triclinic modified chlorite

atom-atom	Distance (Å)	atom-atom	Distance (Å)	atom-atom-atom	Angle° (°)
<b>Tetrahedral sites</b>					
T1-01	1.652(8)	01-03	2.73(1)	01-T1-03	110.8(3)
T1-03	1.662(6)	01-04	2.73(1)	01-T1-04	110.0(3)
T1-04	1.678(5)	01-05	2.71(1)	01-T1-05	110.2(4)
T1-05	1.657(7)	03-04	2.705(7)	03-T1-04	108.2(3)
Mean	1.662	03-05	2.695(9)	03-T1-05	108.6(4)
		04-05	2.716(6)	04-T1-05	109.0(3)
T2-02	1.635(6)	02-03	2.714(9)	02-T2-03	110.5(3)
T2-03	1.667(6)	02-04	2.709(9)	02-T2-04	110.1(3)
T2-04	1.670(6)	02-05	2.71(1)	02-T2-05	110.0(4)
T2-05	1.672(6)	03-04	2.711(8)	03-T2-04	108.6(3)
Mean	1.661	03-05	2.719(8)	03-T2-05	109.0(4)
		04-05	2.711(6)	04-T2-05	108.4(4)
<b>Octahedral sites</b>					
shared edges					
M1-01 ×2	2.088(5)	01-02 ×2	2.809(8)		
M1-0 02 ×2	2.101(4)	01-06 ×2	2.795(8)		
M1-06 ×2	2.087(5)	02-06 ×2	2.805(8)		
Mean	2.092	unshared edges			
		01-02 ×2	3.108(5)		
		01-06 ×2	3.102(5)		
		02-06 ×2	3.109(5)		
shared edges					
M2-01	2.091(5)	01-01*	2.799(8)		
M2-01*	2.089(5)	01-06*	2.795(8)		
M2-02	2.094(5)	01*-02	2.809(8)		
M2-02*	2.099(5)	02-02*	2.831(7)		
M2-06	2.087(5)	02*-06	2.805(8)		
M2-06*	2.084(5)	06-06*	2.774(8)		
Mean	2.091	unshared edges			
		01-02	3.099(5)		
		01-06	3.104(4)		
		01*-02*	3.107(5)		
		01-06*	3.107(4)		
		02-06	3.108(5)		
		02*-06*	3.097(5)		
<b>Interlayer sites</b>					
I1-I4*	1.84(1)	I4*-I1-I5*	117(1)		
I1-I5*	1.82(2)	I4*-I1-I6*	117(1)		
I1-I6*	1.80(2)	I5-I1-I6*	117.1(6)		
I1-†I5	2.33(2)	I4*-I1-†I5	107.6(7)		
		I5*-I1-†I5	96.3(8)		
		I6*-I1-†I5	95.8(8)		
I2-I4*	1.82(1)	I4*-I2-I5*	116.4(6)		
I2-I5*	1.83(1)	I4*-I2-I6*	117.5(6)		
I2-I6*	1.83(1)	I5*-I2-I6*	116.5(6)		
I2-†I6	2.30(2)	I4*-I2-†I6	108.8(7)		
		I5*-I2-†I6	96.0(7)		
		I6*-I2-†I6	96.3(7)		
I3-I4	1.82(1)	I4-I3-I5	120.2(6)		
I3-I5	1.80(1)	I4-I3-I6	120.2(6)		
I3-I6	1.80(1)	I5-I3-I6	119.6(6)		
I4-I1*	1.84(1)	I1*-I4-I2*	112.6(8)		
I4-I2*	1.82(1)	I1*-I4-I3*	115.9(8)		
I4-I3*	1.82(1)	I2*-I4-I3*	115.3(5)		
I4-†04	2.27(1)	I1*-I4-†04	97.3(6)		
		I2*-I4-†04	98.0(6)		
		I3*-I4-†04	115.0(7)		
I5-I1*	1.82(2)	I1*-I5-I2*	119.0(6)		
I5-I2*	1.83(1)	I1*-I5-I3*	120.9(6)		
I5-I3*	1.80(1)	I2*-I5-I3*	119.0(6)		
I5-†I1	2.33(1)	I1*-I5-†I1	83.7(8)		
I5-†03	2.57(2)	I2*-I5-†I1	83.4(8)		
		I3*-I5-†I1	92.3(7)		
I6-I1*	1.80(2)	I1*-I6-I2*	118.8(6)		
I6-I2*	1.83(1)	I1*-I6-I3*	119.3(5)		
I6-I3*	1.80(1)	I2*-I6-I3*	121.0(6)		
I6-†I2	2.30(2)	I1*-I6-†I2	84.8(7)		
I6-†05	2.59(2)	I2*-I6-†I2	83.7(7)		
		I3*-I6-†I2	92.2(7)		

\* Atom position derived by  $(\bar{x}, \bar{y}, \bar{z})$  transformation.

† Second-nearest neighbor atom occurring out-of-plane, see text.

**TABLE 2b.** Select interatomic distances and angles for monoclinic modified chlorite

atom-atom	Distance (Å)	atom-atom	Distance (Å)	atom-atom-atom	Angle° (°)
<b>Tetrahedral site</b>					
T1-01	1.650(6)	01-02	2.739(10)	01-T-02	110.8(4)
T1-02	1.679(4)	01-03	2.725(8)	01-T-03	110.7(3)
T1-03	1.663(5)	01-03*	2.738(8)	01-T-03*	110.9(3)
T1-03*	1.675(5)	02-03	2.701(5)	02-T-03	107.9(3)
Mean	1.667	02-03*	2.712(5)	02-T-03*	108.0(3)
		03-03*	2.711(6)	03-T-03*	108.6(3)
<b>Octahedral sites</b>					
shared edges					
M1-01 ×4	2.096(4)	01-01* ×2	2.823(7)		
M1-04 ×2	2.089(5)	01-04 ×4	2.799(8)		
Mean	2.094	unshared edges			
		01-01* ×2	3.099(4)		
		01-04 ×4	3.112(4)		
shared edges					
M2-01 ×2	2.090(4)	01-01*	2.823(7)		
M2-01* ×2	2.093(4)	01-01* ×2	2.811(7)		
M2-04 ×2	2.080(5)	01-04 ×2	2.799(8)		
Mean	2.088	01-04-04*	2.773(10)		
unshared edges					
		01-04 ×2	3.096(3)		
		01*-04 ×2	3.091(4)		
		01-01* ×2	3.099(4)		
<b>Interlayer sites</b>					
I1-I2	1.836(1)	I2-I1-I2	112.2(6)		
I1-I2*	1.836(1)	I2-I1-I4	116.0(5)		
I1-I4	1.800(1)	I4-I1-I2	116.0(5)		
I1-†02	2.267(17)	I4-I1-†02	115.3(7)		
		I2-I1-†02	97.2(5)		
I2-I1	1.84(1)	I1-I2-I3	117.1(6)		
I2-I3	1.81(1)	I1-I2-I3*	116.3(6)		
I2-I3*	1.81(1)	I3-I2-I3*	117.2(6)		
I2-†I3*	2.34(2)	I1-I2-†I3	107.9(7)		
		I3-I2-†I3	96.3(6)		
		I3*-I2-†I3	96.7(6)		
I3-I2	1.81(1)	I2-I3-I4	119.8(5)		
I3-I2*	1.81(1)	I2-I3-I2*	119.5(5)		
I3-I4	1.812(9)	I2*-I3-I4	119.4(6)		
I3-†I2*	2.34(2)	I2-I3-†I2*	83.7(6)		
I3-†03	2.56(1)	I2*-I3-†I2*	83.3(6)		
		I4-I3-†I2*	91.3(6)		
I4-I1	1.80(1)	I1-I4-I3	120.5(4)		
I4-I3	1.812(9)	I1-I4-I3*	120.5(4)		
I4-I3*	1.812(9)	I3-I4-I3*	118.9(8)		

\* Atom position derived by one or more symmetry transformations.

† Second-nearest neighbor atom occurring out-of-plane, see text.

ions. Thus, the resulting chemical composition of the modified chlorite structure is:  $(\text{Mg}_{2.97}\text{Al}_{0.03})(\text{Si}_{3.02}\text{Al}_{0.98})\text{O}_{10}(\text{OH})_2$   $(\text{Mg}_{1.98}\text{Al}_{0.69}\text{Cr}_{0.23}\text{Fe}_{0.04}^{3+}\text{Fe}_{0.04}^{2+}\text{Ni}_{0.02}\Sigma_{\Sigma=3}\text{O}_3)$ .

### Interlayer planes

There are two, nearly planar, sets of atoms located in the region between the 2:1 layers ("interlayer" region). Interlayer sites (designated as "I" in Tables 1 and 2) are not distinguishable as being either cation ( $\text{R}^{2+}$ ,  $\text{R}^{3+}$ ) or oxygen sites. The most probable local structure for each plane consists of cations in threefold coordination with oxygen, with an ordering pattern as illustrated in Figure 1. Although strong electrostatic interactions may fix cation and oxygen positions within each plane, cation-oxygen disorder may occur within each plane because the occupancy of I sites from unit cell to unit cell along the *c* axis (i.e., alternating with 2:1 layers) is not fixed. Unlike the

parent chlorite phases where hydrogen bonding and electrostatic interactions establish linkages between the 2:1 layer and adjacent portions, dehydroxylation upon heat-treatment weakens such linkages considerably.

The interlayer planes are illustrated in Figures 2 and 3. Figure 2 shows a perspective view to illustrate that the I sites are only quasi-planar. For example, in the triclinic form, I2 and I4 vary from the average plane by 0.223 Å and 0.322 Å, respectively (Table 3). Examination of I-I-I angles within the plane (Table 2) show significant deviations from the ideal 120° angles expected for (planar) threefold coordination with a central cation; in the triclinic form, for example, the variations range from 112.6 to 120.2°.

At high temperatures, where the unit cell is more expanded, these planes are probably more fully extended and more planar. Thus, we suggest that the interlayer planes "crumple" upon cooling. Otherwise, if these planes were to remain rigid and planar, an incommensurate structure would form between the interlayer planar structure and the adjacent 2:1 layers. Energetically, an incommensurate arrangement appears to be less favorable than "crumpled" layers.

### 2:1 layer

The 2:1 layers of the two heat-treated phases are remarkably similar. The octahedra (triclinic form: M1 = 2.092 Å, M2 = 2.091 Å; monoclinic form: 2.094 Å, 2.088 Å) are identical in size, within experimental error, as are the corresponding tetrahedra (triclinic form: T1 = 1.662 Å, T2 = 1.661 Å; monoclinic form: 1.667 Å). However, the octahedra (Phillips et al. 1980) in the heat-treated *Iib-4* sample are slightly smaller in the par-

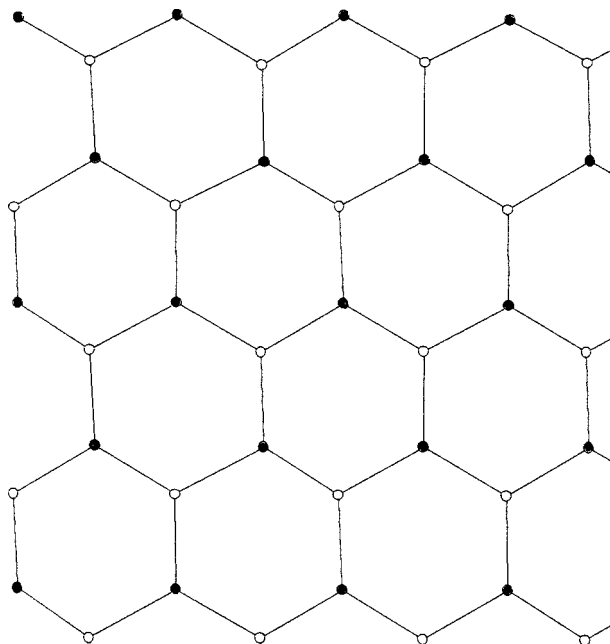


**FIGURE 1.** Proposed ordering pattern for interlayer (001) plane. The [100] direction points down and the [010] direction points to the right. Solid circles represent R cations and open circles are oxygen atoms.

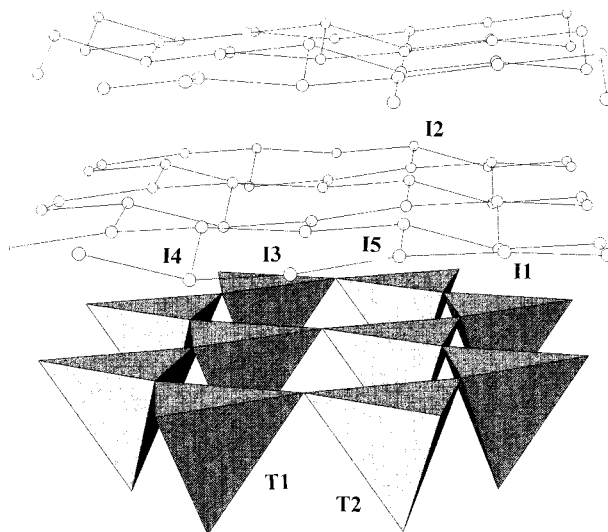


**FIGURE 2.** Perspective view of the triclinic modified chlorite structure approximately down the [100] direction to illustrate the quasi-planar configuration of the interlayer planes (I sites). The upper portion of the 2:1 layer (T1, T2 tetrahedra) and both interlayer planes are illustrated.

ent (M1: 2.075 Å, M2: 2.076 Å) than in the room-temperature, heat-treated derived material. Similarly, the tetrahedra are also smaller in the parent (T1: 1.654 Å, T2: 1.653 Å) than in the room-temperature, heat-treated derived material. The differences in the octahedral sites for the triclinic forms are 0.016 Å, marginally significant considering estimated standard deviations of 0.004 Å (Phillips et al. 1980) and 0.005 Å (this study). Since the octahedral sites of the heat-treated sample are larger than the parent, oxidation reactions can be ruled out. These results indicate that the octahedra are occupied primarily by Mg. The tetrahedral rotation angle ( $\alpha$ ) for each structure, which is a measure of lateral misfit of the tetrahedral and octahedral sheets, compares closely ( $7.2 \pm 0.3$  vs.  $7.6 \pm 0.2^\circ$ ), and this suggests near identical chemistries for the 2:1 layers.

### Polytypism of the starting phases and the effect on the products

The structures of the *Iib-2* and *Iib-4* polytypes play an important role in determining the structural differences between the two product phases that result from heating, and thus, the differences between the two parent phases are discussed here briefly. A displacement vector may be defined as extending from the OH in the center of the lower silicate ring in the 2:1 layer to the OH in the center of the upper adjacent ring across the octahedra within the same 2:1 layer. Within the 2:1 layer, there is a stagger of  $a/3$  between the upper tetrahedral sheet relative to the lower tetrahedral sheet (Bailey and Brown 1962). For one-layer polytypes with monoclinic symmetry (e.g., *Iib-2*), the displacement vector parallels the stagger direction with both directions in the mirror plane, and it is for this reason that the overall symmetry of the structure is monoclinic. In contrast, for polytypes with triclinic symmetry (e.g., *Iib-4*), the

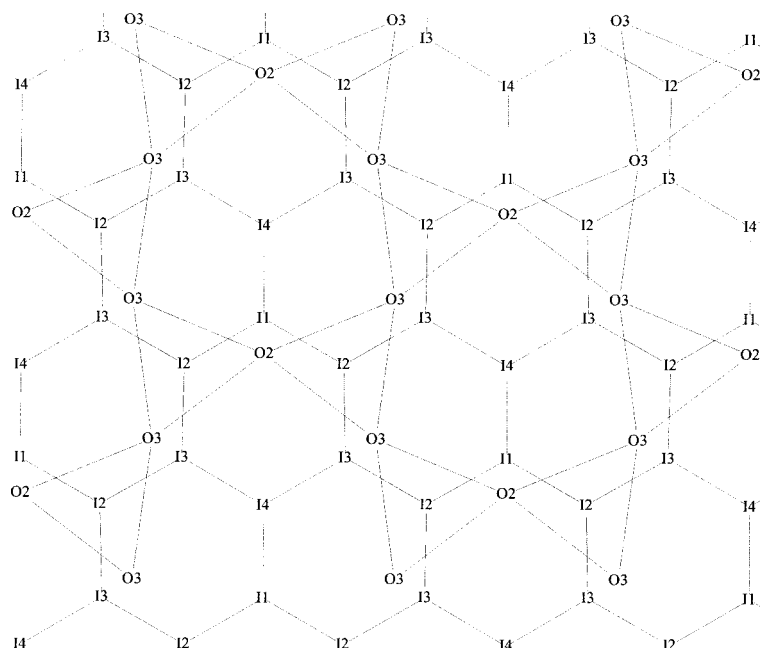


**FIGURE 3.** Projection down  $c^*$  of the monoclinic modified chlorite structure showing the interlayer plane (I sites) and adjacent tetrahedral sheet (shaded triangles). The tetrahedral sheet is the upper portion of the 2:1 layer. The [100] direction points down and the [010] direction points to the right.

**TABLE 3.** Structural parameters for modified chlorite

Parameter	Monoclinic form heat-treated <i>I/b-2</i>	Triclinic form heat-treated <i>I/b-4</i>
$\alpha^{\circ}$	$7.62 \pm 0.2$	$7.15 \pm 0.3$
$\tau^{\circ}$	110.8	T1: 110.3 T2: 110.2
$\psi^{\circ}$ : M1	58.95	59.01
M2	58.85	59.00
$\beta_{\text{ideal}}^{\circ}$	97.21	97.26
Sheet thickness (Å)		
Tetrahedral	2.250	2.228
Octahedral	2.160	2.154
Interlayer thickness (Å)	7.493	7.495
Interlayer planar deviation (Å)	$\pm 0.264$	$\pm 0.273$

\* Tetrahedral rotation is calculated from  $\alpha = 1/2|120^{\circ} - \text{mean } 0b-0b-0b|$  angle.

† The tetrahedral angle is defined as  $\tau = \angle \text{O}_{\text{apical}}\text{-Si-O}_{\text{basal}}$ . The ideal value is  $109.47^{\circ}$ .

‡ The mean octahedral angle, ideally  $54.73^{\circ}$ , is calculated from  $\cos \psi = \text{oct. thickness}/2(M-0.0H)$ .

§  $\beta_{\text{ideal}} = 180^{\circ} - \cos^{-1}(a/3c)$ .

stagger direction is not parallel to the displacement vector. These differences remain upon dehydroxylation of the interlayer. Two important points are (1) because of the different displacement directions in the 2:1 layers between the two polytypes, the OH arrangements relative to the interlayer are not the same and (2) the different displacement directions in the 2:1 layer are not reflected in the polytype symbol, although differences are indicated by designating the space group symmetry.

The polytype symbol emphasizes the differences between the 2:1 layer and the interlayer. For example, the “*I*” symbol indicates that the interlayer cations occupy octahedral positions to produce an “octahedral slant” that is opposite from the slant in the 2:1 layer (Bailey and Brown 1962). The “*b*” symbol indicates that the interlayer sheet is ringed in a fixed way with respect to the underlying silicate ring so that hydrogen bonds

may form, and the “-2” or “-4” symbol indicates the position of the overlying 2:1 layer over the interlayer to form hydrogen bonds. These symbols, however, have no relevance to the heat-treated samples, since the “interlayer” is not comprised of octahedra-coordinating cations and dehydroxylation eliminates the requirement for hydrogen bond contacts involving donor and acceptor O atoms.

The placement of the interlayer plane of I sites relative to the tetrahedral sheet below (Fig. 3) shows that every tetrahedron has an associated I site nearly superposed directly over the tetrahedral cation (triclinic form: I1-T1, I2-T2; monoclinic form: I2-T). All I-T distances within both forms are near 3.3 Å. These distances are sufficiently close that Coulombic interactions would be expected to occur, although thermal effects (i.e., dynamic atom displacements) increase the probability of disorder (see the section below). Also, note from Figure 3 that each bridging oxygen atom has an associated I site, and an I site exists near the center of the ditrigonal ring. Therefore, the stacking of the interlayer planes in the two forms are very similar, with differences relating to second and third nearest neighbor effects.

### Differences in interlayer sites and the potential for cation-anion ordering

Without hydrogen bonding between the 2:1 layer and adjacent interlayer planes, the only interactions between these structural units are electrostatic. Because some I sites have close second nearest-neighbor distances in the adjacent interlayer plane and within the 2:1 layer, it seems likely from charge-balance considerations that some out-of-plane interactions exist. For example, distances between adjacent I sites located on neighboring interlayer planes are short, about 2.3 Å [monoclinic: I2-I3\* = I3-I2\* = 2.34(2) Å; triclinic: I1-I5 = 2.33(2), I2-I6 = 2.30(2) Å]. It would be expected that if an R cation occupies an I site in the lower interlayer plane (e.g.,  $z$  at near

0.41), then Coulombic interactions would favor that the I site immediately adjacent on the other plane ( $z$  at near 0.59) would be occupied by an oxygen atom. Thus, electrostatic forces exist that should promote ordering of cations in fixed positions in the two interlayer planes. Likewise, certain I sites have relatively short second nearest-neighbor distances to the basal oxygen plane of the 2:1 layer [monoclinic: I1-O2 = 2.27(2), I3-O3 = 2.56(1) Å; triclinic: I4-O4 = 2.27(1) Å], suggesting also that electrostatic interactions between these sites and the 2:1 layer exist. These I sites are more closely coordinated to oxygen atoms and would be expected to be occupied by an R cation. Following the same reasoning, I sites that superpose over T sites (see above) would favor oxygen atom occupancies. Based on electrostatic considerations of out-of-plane interactions, note that I sites most favorable for oxygen occupancy alternate within the plane with I sites most favorable for cation occupancy. Thus, both out-of-plane and in-plane interactions appear to favor the ordering scheme proposed in Figure 1.

The fact that cation and anion ordering does not occur in the interlayer even though favorable electrostatic interactions exist at room temperature suggests that (1) there are structural factors at high temperature that promote disorder and (2) there may be conditions of formation that promote order. The model presented here in which the interlayer planes are expanded at high temperature and crumple as the structure cools, suggests a driving force for cation and anion ordering, since crumpling brings electrostatic interactions between I sites and out-of-plane neighbors favorable for ordering into play. However, slow cooling or annealing for long periods at lower temperatures may be required for ordering to occur. To prevent back reactions, our crystals were quenched rapidly from 650 °C and thus, our experimental protocol favored cation and anion disorder.

Using material from the same locality as the starting material used here, Nelson and Guggenheim (1993) determined the crystal structure of triclinic clinocllore-*I1b-4* at 550 °C. Therefore, it is possible to use the structural model of the high-temperature clinocllore 2:1 layer (Nelson and Guggenheim 1993), in combination with the interlayer model as derived in this study, to understand how the two portions of the structure interact as a function of temperature and why cation and anion disorder is favored in the interlayer at high temperatures.

At 550 °C, the tetrahedral rotation angle of triclinic clinocllore-*I1b-4* is 4.6° (c.f. 7.15° for heated-treated clinocllore at room temperature). The rotation angle is the measure of in-plane rotation of the silica tetrahedra, and is generally considered related to the misfit between the tetrahedral sheet and the octahedral sheet of the 2:1 layer. With increasing temperature, the octahedral sheet expands more than the tetrahedral sheet and thus, the tetrahedra of the silicate ring rotate to compensate. A smaller rotation angle indicates that the tetrahedral ring expands. At high temperatures and after dehydroxylation, the basal oxygen atoms are considerably further away from the I sites (compared to room temperature) in adjacent interlayer planes because (1) tetrahedral rotation occurs with a direction of rotation at higher temperatures away from the basal oxygen atoms, (2) the interlayer planes are more expanded, and (3) hydrogen bonding cannot inhibit basal oxygen atom movement. Thus, cation and anion disorder in the

interlayer at high temperature is not only a function of dynamic (thermal) atom displacements, but also a lessening of electrostatic interactions.

## CONCLUDING REMARKS

Upon heating at elevated temperatures to produce dehydroxylation of the interlayer, sixfold-coordinated cations (Mg, Al, Cr) in the interlayer of the Day Book Body chlorite become threefold-coordinated with oxygen atoms and, likewise, oxygen atoms become threefold-coordinated with cations. The structure is readily quenchable and persists at room temperature but it does not occur in nature, probably because of the long-term instability relating to the low coordination numbers. Two quasi-planar sets of atoms exist in the interlayer between the 2:1 layers, but it is not possible to distinguish between cation and anion positions in the interlayer. We believe that at high temperatures, these quasi-planes are more fully extended. Upon cooling, however, the planes crumple and the cations can more closely approach higher-order nearest neighbor oxygen atoms. It is suggested that with appropriate cooling rates, the free energy of the system would be minimized significantly by cation and anion ordering. The driving force of the proposed ordering process involves the electrostatic interactions of the interlayer cations and anions as they move closer to the higher-order nearest neighbor coordinating ions. It is unclear, however, if the driving force for ordering at very slow cooling rates would prevail over the instability of the low coordinated interlayer sites (and resulting decomposition). This paper establishes the basis for further work.

## ACKNOWLEDGMENT

We thank Phil Slade, CSIRO, Adelaide, for his review.

## REFERENCES CITED

- Bai, T.-B., Guggenheim, S., Wang, S.-J., Rancourt, D.G., and Koster van Groos, A.F. (1993) Metastable phase relations in the chlorite-H<sub>2</sub>O system. *American Mineralogist*, 78, 1208–1216.
- Bailey, S.W. and Brown, B.E. (1962) Chlorite polytypism: I. Regular and semi-random one-layer structures. *American Mineralogist*, 47, 819–850.
- Brindley, G.W. and Ali, S.Z. (1950) X-ray study of thermal transformations in some magnesium chlorite minerals. *Acta Crystallographica*, 3, 25–30.
- Brindley, G.W. and Chang, T.-S. (1974) Development of long basal spacings in chlorites by thermal treatment. *American Mineralogist*, 59, 152–158.
- Cromer, D.T. and Mann, J.B. (1968) X-ray scattering factors computed from numerical Hartree-Fock wave functions. *Acta Crystallographica*, A24, 321–324.
- Moore, D.M. and Reynolds, R.C. Jr. (1989) X-ray Diffraction and the identification and analysis of clay minerals. Oxford University Press, Oxford, 332 p.
- Nelson, D.O. and Guggenheim, S. (1993) Inferred limitations to the oxidation of Fe in chlorite: A high-temperature single-crystal X-ray study. *American Mineralogist*, 78, 1197–1207.
- Phillips, T.L., Loveless, J.K., and Bailey, S.W. (1980) Cr<sup>3+</sup> coordination in chlorites: a structural study of ten chromian chlorites. *American Mineralogist*, 65, 112–122.
- Sales, K.D. (1987) Atomic scattering factors for mixed atom sites. *Acta Crystallographica*, A43, 42–44.
- Siemens (1990) SHELXTL PLUS 4.0. Siemens Analytical X-Ray Instruments, Inc., Madison, Wisconsin.
- Villieras, F., Yvon, J., Cases, J.M., de Donato, P., Lhote, F., and Baeza, R. (1994) Development of microporosity in clinocllore upon heating. *Clays and Clay Minerals*, 42, 679–688.
- Zhan, W. and Guggenheim, S. (1995) The dehydroxylation of chlorite and the formation of topotactic product phases. *Clays and Clay Minerals*, 43, 622–629.
- Zheng, H. and Bailey, S.W. (1989) The structures of intergrown triclinic and monoclinic *I1b* chlorites from Kenya. *Clays and Clay Minerals*, 37, 308–316.

MANUSCRIPT RECEIVED SEPTEMBER 17, 1998

MANUSCRIPT ACCEPTED MAY 4, 1999

PAPER HANDLED BY R.A. EGGLETON